

## Highlights

### **Experimental Results of Underwater Sound Speed Profile Inversion by Few-shot Multi-task Learning**

Wei Huang,Fan Gao,Junting Wang,Hao Zhang

- To achieve good accuracy performance of SSP inversion under few-shot learning situation, we propose the MTL approach. Through learning on multi-task (different kinds of SSPs), the common features of SSPs are extracted to accelerate the convergence rate of the model on any given task with less training times, so as to weaken the over-fitting effect.
- To verify the feasibility of MTL, a deep-ocean experiment for SSP inversion is conducted. The accuracy performance of SSP inversion is evaluated based on measured data and compared with state-of-the-art methods.
- To solve the problem of limited coverage of XCTD, we propose a fast sound speed distribution estimation method based on MFP with EOF decomposition, which could accurately extend the SSPs to deeper layers.

# Experimental Results of Underwater Sound Speed Profile Inversion by Few-shot Multi-task Learning<sup>★</sup>

Wei Huang<sup>a</sup>, Fan Gao<sup>b</sup>, Junting Wang<sup>b</sup> and Hao Zhang<sup>a,\*</sup>

<sup>a</sup>Ocean University of China, Qingdao 266100, China

<sup>a</sup>Shandong University at Weihai, Weihai 264200, China

---

## ARTICLE INFO

### Keywords:

keyword-1 Sound Speed Profile (SSP)

keyword-2 multi-task learning (MTL)

keyword-3 few-shot learning

## ABSTRACT

Underwater Sound Speed Profile (SSP) distribution has great influence on the propagation mode of acoustic signal, thus the fast and accurate estimation of SSP is of great importance in building underwater observation systems. The state-of-the-art SSP inversion methods include frameworks of matched field processing (MFP), compressive sensing (CS), and feedforward neural networks (FNN), among which the FNN shows better real-time performance while maintain the same level of accuracy. However, the training of FNN needs quite a lot historical SSP samples, which is difficult to be satisfied in many ocean areas. This situation is called few-shot learning. To tackle this issue, we propose a multi-task learning (MTL) model with partial parameter sharing among different training tasks. By MTL, common features could be extracted, thus accelerating the learning process on given tasks, and reducing the demand for reference samples, so as to enhance the generalization ability in few-shot learning. To verify the feasibility and effectiveness of MTL, a deep-ocean experiment was held in April 2023 at the South China Sea. Results show that MTL outperforms the state-of-the-art methods in terms of accuracy for SSP inversion, while inherits the real-time advantage of FNN during the inversion stage.

---

## 1. Introduction

Underwater observation system has become a good way to provide positioning, navigation, and timing (PNT) services in recent years [10, 11, 24]. Communication and localization are the two most important technological basis for underwater observation systems, and because of the attenuation problems, the sound wave becomes the main carrier for long-distance signal transmission in underwater environment. However, the uniformly distribution of sound speed can lead to great Snell effect, which means the signal will propagate non-straightly. So the sound field information will be dynamically changed such as signal propagation time or received signal strength [19]. Fortunately, if the sound speed distribution could be obtained, the sound field distribution can be accurately estimated according to ray theory [26] or normal mode theory [27, 34], thus the accuracy of ranging and positioning could be improved [4, 23, 42].

With a same range scale, the variation of sound speed in the vertical direction is much greater than that in the horizontal direction, so sound speed profiles (SSPs) are usually used to represent the distribution of sound speed [19]. Recently, many SSP inversion approaches leveraging sound field information have been proposed in underwater wireless sensor networks for inverting SSPs. The research of novel SSP inversion methods is very promising because they are more automatic and less labor-time-consuming than the measurement of SSPs by sound velocity profiler (SVP) or conductivity-temperature-depth (CTD) systems [45, 15].

The state-of-the-art SSP inversion frameworks contains matched field processing (MFP) [39], compressive sensing (CS) [6, 22] and feedforward neural networks (FNN) [36, 15]. The estimation of real-time SSP is a difficult work because, to the best of our knowledge, there is no empirical formula that could establish the mapping relationship from sound field information to the SSP. Nevertheless, based on ray theory, Tolstoy proposed a MFP framework combining empirical orthogonal function (EOF) decomposition for SSP inversion. In this work, the establishment

---

<sup>★</sup>This document is the results of the research project funded by Natural Science Foundation of Shandong Province (ZR2023QF128), China Postdoctoral Science Foundation (2022M722990), Qingdao Postdoctoral Science Foundation (QDBSH20220202061), National Natural Science Foundation of China (NSFC:62271459), National Defense Science and Technology Innovation Special Zone Project: Marine Science and Technology Collaborative Innovation Center (22-05-CXZX-04-01-02), and the Fundamental Research Funds for the Central Universities, Ocean University of China (202313036)..

\*Corresponding author

✉ hw@ouc.edu.cn (W. Huang); gaofan@stu.edu.cn (F. Gao); wjts2015@163.com (J. Wang); zhanghao@ouc.edu.cn (H. Zhang)

ORCID(s): 0000-0002-8284-2310 (W. Huang)

of direct mapping from the sound field to the sound speed distribution is avoided. Therefore, MFP has become the mainstream framework for SSP inversion for a long time.

The optimal solution of [39] is searched traversely, so the computational complexity of MFP is quite high. To accelerate the SSP inversion process, many researchers have adopted heuristic algorithms into the search for optimal solutions, such as the simulated annealing algorithm [47], the particle swarm optimization (PSO) algorithm [46, 48], and the genetic algorithm [38, 37]. However, the core idea of heuristic algorithm is based on Monte Carlo, so the heuristic algorithm still requires a lot of iterative searches to determine the matching items. To improve the efficiency of SSP inversion, [6, 22] proposed a CS framework for SSP inversion, which establishes a dictionary to directly map the sound field information to sound speed distribution. Compared with MFP, the CS framework only requires a few iterations to train the dictionary, so that the computational complexity can be reduced. However, the mapping from sound field to sound speed distribution is linearly simplified through the first-order Taylor expansion, which sacrifices the accuracy performance.

Recently, Bianco et al. [2] did a comprehensive survey that machine learning has gained broad application prospects in the field of underwater acoustics, such as seafloor characterization [25], range estimation [21], geoacoustic inversion [29], and SSP inversion [36, 15, 17]. In our early work [15], we proposed a FNN structure for SSP inversion with the assist of ray theory. The model training can be completed offline in advance. After the model converging, only one round of forward propagation is required to invert the SSP when feeding the measured sound field data into the network. Thus, the inversion efficiency of the FNN model is significantly higher than that of the MFP and CS models. To improve the robustness of FNN models under noise interference, we proposed an auto-encoder feature-mapping neural network (AEFMNN) in [17]. By denoising and reconstructing sound field information, hidden features with stronger anti-interference ability are extracted, thereby improving the accuracy of SSP inversion.

The performance of MFP, CS, or FNN models all relies on a large amount of historical SSPs as references. However, due to the high economic and labor costs of historical SSPs measured by CTD or SVP, the reference SSPs available in many spatio-temporal ocean areas are so limited that there may be insufficient reference data for model training, making the model prone to be overfitting. Many approaches for few-shot learning surveyed in [40, 14] have been proposed to solve the overfitting problem, such as regularization [13], training dataset expanding with generative adversarial networks [20], multi-task learning (MTL) [31, 43], transfer learning (TL) [41, 28], and meta-learning approaches [40, 14, 12].

Regularization establishes a way to limit the model scale by narrowing down the values of weight parameters (L2 norm) or making the model parameters sparse (L1 norm). Thus, the ability of fitting complex relationships of the model is weakened so that overfitting problem could be reduced. Training dataset expanding aims to enrich the training dataset that could represent the whole situation of target domain, however, if the original training data are unable to uniformly represent the regional distribution of sound speed, the expanded training dataset cannot compensate for this shortcoming, thus the model is still prone to be overfitting. MTL jointly learns several related tasks, while TL uses past experience of a source task to improve learning on a new task by transferring the model's prior parameter in [5] or the feature extractor from the solution of a previous task in [44]. However, the generalization ability on new tasks of these two models is still insufficient due to excessive retention of old task information.

For solving the few-shot learning problem in SSP inversion, we propose a multi-task learning (MTL) method to accurately estimate the regional SSP distribution. The core idea is to extract the common features from different kinds of SSP clusters via a partial parameter shared neural network, which forms a set of initialization parameters for the model of inversion task. When training on the few-shot samples of the task, the learning rate is dynamically adjusted based on the distance of spatio-temporal information between the reference SSP sample and the task mission. Through MTL, the convergence rate of the model could be accelerated and the sensibility to the input data could be retained, so that the model will not be over trained on few-shot task samples. To demonstrate the effectiveness of MTL, we conducted a deep-ocean experiment in the South China Sea in April 2023. The contribution of our paper can be concluded as:

- To achieve good accuracy performance of SSP inversion under few-shot learning situation, we propose the MTL approach. Through learning on multi-task (different kinds of SSPs), the common features of SSPs are extracted to accelerate the convergence rate of the model on any given task with less training times, so as to weaken the over-fitting effect.
- To verify the feasibility of MTL, a deep-ocean experiment for SSP inversion is conducted. The accuracy performance of SSP inversion is evaluated based on measured data and compared with state-of-the-art methods.

- To solve the problem of limited coverage of XCTD, we propose a fast sound speed distribution estimation method based on MFP with EOF decomposition, which could accurately extend the SSPs to deeper layers.

The rest of this paper is organized as follows. In Sec. 2, we propose the MTL model for SSP inversion. In Sec. 3, we introduce the scenarios and processes of the deep-ocean experiment for SSP inversion. Experimental results are discussed in Sec. 4, and conclusions are given in Sec. 5.

## 2. MTL Model for SSP Inversion

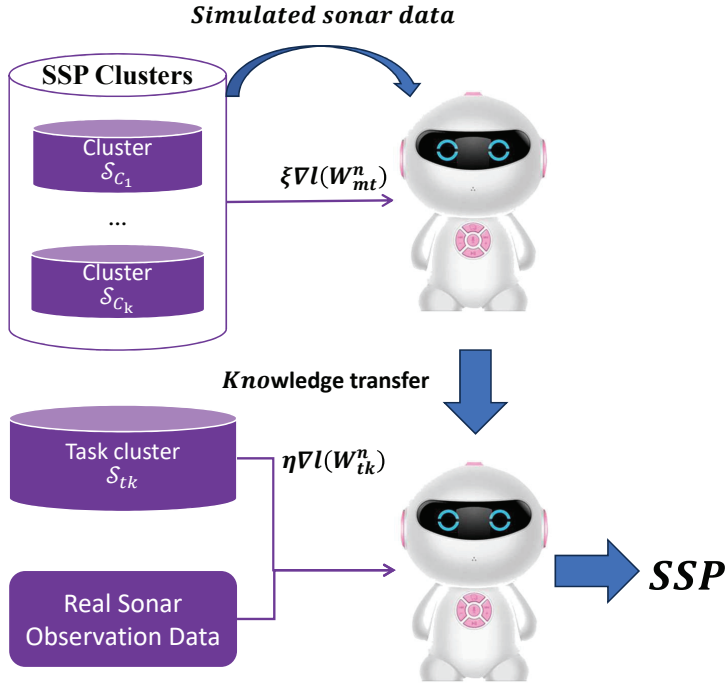


Figure 1: MTL SSP inversion model.

To improve the SSP inversion accuracy under few-shot learning situation, we propose a MTL model, in which different types of SSPs sampled in different spatio-temporal regions will be used for pretraining. While for training on the task group, the learning rate will be dynamically adjusted according to the distance of spatio-temporal information between the reference SSP and the inversion task. The illustration of MTL training and SSP inversion is shown in Fig.1.

The MTL model is a three-layers FNN proposed in our previous work [15] as shown in Fig.2. There is a multi-task learner and a task learner in our model. The input layer is signal propagation time sequence, and the number of input layer neurons is consistent with the sonar observation data collected by the transmitting and receiving nodes, and the detailed sonar observation data collection process will be given in the ocean experiment section. The output layer is the inverted SSP, while the label data is the training SSP. For pretraining, the weights between the input layer and the hidden layer are shared, while the weights between the hidden layer and the output layer are unique related to the training task. During each epoch,  $n$  kinds of SSPs with  $V$ -shot SSPs for each are randomly chosen from the whole SSP clusters for training the multi-task model, which aims to learn a good set of initialization parameters for the model's shared parameters. Thus, the task learner initialized by the multi-task learner could be quickly converged with a few training times on the task SSP training set.

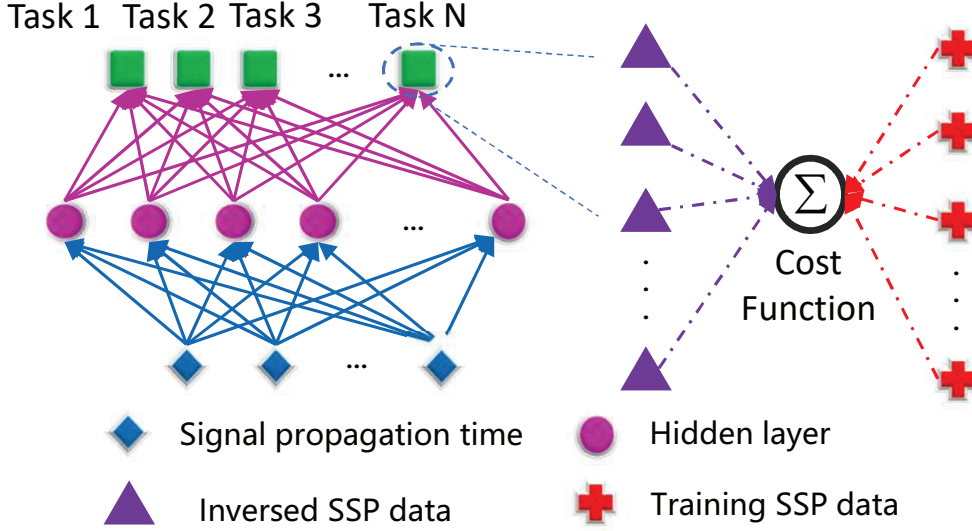


Figure 2: Structure of neural networks in MTL.

## 2.1. Label SSP Data Preparation

The training historical SSP data for the mutli-task learner could be either clustered manually or intelligently. In our pervious work [16], we propose a local density clustering method based on Euclidean distance, which can effectively group SSPs with similar distribution even through they are sampled in different spatio-temporal ocean regions.

For a given SSP inversion task, a small number of reference SSPs having the similar distribution with the target task are still necessary for training the task learner. However, the sound speed distribution of the target task is not a prior information, therefore, the potential reference SSPs can not be selected according to the distribution features of SSPs. In our pervious work [16], we propose a method to find proper traning data for a given task according to its spario-temporal information.

In this paper, a spatio-temporal distance parameter  $\phi$  is designed to describe the similarity between the sampling region of a reference SSP and the task, which can be expressed as:

$$\phi = \lambda_{tk} * \phi_{\alpha} + (1 - \lambda_{tk}) * \phi_{\beta}, \quad (1)$$

where  $\phi_{\alpha}$  is the time difference,  $\phi_{\beta}$  is the location difference, and  $0 \leq \lambda_{tk} \leq 1$  is a factor to balance  $\phi_{\alpha}$  and  $\phi_{\beta}$ . The time difference  $\phi_{\alpha}$  is calculated by:

$$\phi_{\alpha} = \begin{cases} |\alpha_{tk} - \alpha_r|, & \text{if } |\alpha_{tk} - \alpha_r| < 183 \\ 365 + \min(\alpha_{tk}, \alpha_r) - \max(\alpha_{tk}, \alpha_r), & \text{otherwise} \end{cases} \quad (2)$$

where  $\alpha_{tk}$  and  $\alpha_r$  are the time information of SSP inversion task and a random reference SSP of the task learner, respectively. The resolution of sampling time information is defined in days, because SSPs sampled at the same period in different years have almost the same distribution. Therefore, the time information is cyclically encoded that can be described as equation (2).

The space information is defined by the latitude and longitude coordinate of an SSP. The location difference  $\phi_{\beta}$  is calculated by:

$$\phi_{\beta} = \sqrt{(\beta_{tk}^x - \beta_r^x)^2 + (\beta_{tk}^y - \beta_r^y)^2}, \quad (3)$$

where  $\beta_{tk}^x$  and  $\beta_{tk}^y$  represent the longitude and latitude coordinates of task location after coding, respectively, and  $\beta_r^x$  and  $\beta_r^y$  represent the longitude and latitude coordinates of SSP sampling space, respectively. For the Northern Hemisphere, the coded  $\beta^y$  equals to the SSP's latitude coordinate, while  $\beta^x$  is:

$$\beta^x = \begin{cases} |\hat{\beta}^x| - 180, & \text{if } 0^{\circ} E < \hat{\beta}^x < 180^{\circ} E \\ 180 - |\hat{\beta}^x|, & \text{if } 0^{\circ} W < \hat{\beta}^x < 180^{\circ} W \end{cases}, \quad (4)$$

where  $\hat{\beta}^x$  is the original longitude coordinate of the SSP.

Through comparing the spatio-temporal distance between all historical SSPs and the target SSP, the cluster which contains most of the  $\psi$  nearest SSPs will be determined as the reference of the task learner.

## 2.2. Simulation of Signal Propagation Times

Both the training of multi-task learner and the task learner require sound field information as model's input under a given SSP distribution. However, the real measured sound field data are usually collected at the inversion stage, and those sound field data used for model training need to be simulated.

For ocean sensing networks, underwater anchor nodes can be located by a long baseline positioning system composed of several buoys, while the coordinates of buoys can be obtained via the global positioning system (GPS). Let a buoy node be the signal sender, and  $M$  underwater anchor nodes be the receivers, the horizontal propagation distance of the signal with a given SSP  $S = [(s^1, 1), \dots, (s^d, d)]$  can be calculated according to our previous derivation in [17] as:

$$h^m = \frac{s^1}{\cos \theta^{1,m}} \sum_{d=1}^{D-1} \left| \frac{\Delta z_d}{s^{d+1} - s^d} \left( \sqrt{\Gamma_d^m} - \sqrt{\Gamma_{d+1}^m} \right) \right|, \quad (5)$$

$$\Gamma_d^m = 1 - \left( \frac{\cos \theta^{1,m}}{s^1} \right)^2 (s^d)^2,$$

where  $h^m$  is the horizontal signal propagation distance from the buoy to the  $m$ th anchor node,  $d$  is the index of depth layers,  $\theta^{1,m}$  is the initial grazing angle from source to the  $m$ th receiver,  $s^d$  is the sound speed value at depth with index  $d$  and  $\Delta z_d$  is the depth difference of the linear SSP at the  $d$ th layer with depth boundaries of  $d$  and  $d + 1$ .

With known horizontal distance  $h^m$ , the grazing angle of signal from source to each receiver can be searched by equation (5). Then the ideal signal propagation time from source to the  $m$ th receiver can be simulated as:

$$t^m = \sum_{d=1}^{D-1} \left| \frac{\Delta z_d}{s^{d+1} - s^d} \ln \left( \frac{s^d \left( 1 + \sqrt{\Gamma_{d+1}^m} \right)}{s^{d+1} \left( 1 + \sqrt{\Gamma_d^m} \right)} \right) \right|, \quad (6)$$

It can be noticed that  $t^m$  is also a function of the initial grazing angle  $\theta^{1,m}$ .

## 2.3. Training of the Multi-task Learner

The first training phase of MTL that can be conducted offline is the training of multi-task learner. In this stage, the neuron connection parameter of multi-task learner is randomly initialized as  $W_{mt,h}^1$  and  $W_{mt,o}^1$ .  $W_{mt,h}^1$  is the weight matrix between the input layer and the hidden layer, and  $W_{mt,o}^1$  is the weight matrix between the hidden layer and the output layer.

At the beginning of the  $p$ th epoch<sup>1</sup> (or iteration),  $N$  SSP clusters are randomly chosen from the  $K$  available training SSP clusters ( $N \leq K$ ) for training the multi-task learner. In each selected SSP cluster, there are  $V$  training ( $S_v, v = 1, 2, \dots, V$ ). For SSP cluster  $n$ , the  $V$  SSPs are used for one step learning with the cost function defined as:

$$l^{(n)} \left( W_{mt,n}^p \right) = \sum_{v=1}^V \left( \frac{1}{2} \sum_{d=1}^D (s_v^d - \tilde{s}_v^d)^2 + \|W_{mt,n}^p\|_1 \right), \quad W_{mt,n}^p = \left[ W_{mt,h,n}^p, W_{mt,o,n}^p \right], \quad (7)$$

where  $s_v^d$  is the sound speed of the  $v$ th training SSP at depth with index of  $d$ ,  $\tilde{s}_v^d$  is the corresponding inverted sound speed, and  $\|W_{mt,n}^p\|_1$  is the regularization item. Next, the local parameters are updated by back propagation (BP) algorithm [32]:

$$\dot{W}_{mt,n}^p = W_{mt,n}^p - \frac{\xi}{N} \nabla_{W_{mt,n}^p} l^{(n)} \left( W_{mt,n}^p \right), \quad (8)$$

<sup>1</sup>An epoch indicates a round of parameter updating.

where  $\xi$  is the learning rate of the multi-task learner.

For a specified SSP inversion task, the parameters of multi-task learner  $\dot{W}_{mt,h}^P$  is transferred as the initialization for the task learner, thus  $W_{tk,h}^1 = \dot{W}_{mt,h}^P$ , where  $W_{tk,h}^1$  is the weight value matrix between the input layer and the hidden layer. The weight value matrix  $W_{tk,o}^1$  between the hidden layer and the output layer will be initialized randomly. The task learner will be trained on a few reference SSPs by one or a few steps to form the converged model  $\dot{W}_{tk}$ .

Let the  $i$ th reference SSP be  $S_{tk,ri} = \left[ \left( s_{tk,ri}^1, 1 \right), \dots, \left( s_{tk,ri}^d, d \right) \right]$ ,  $d = 1, 2, \dots, D$  with coded sampling location as  $\left( \beta_{tk,ri}^x, \beta_{tk,ri}^y \right)$  and time information as  $\alpha_{tk,ri}$ , so the spatio-temporal distance  $\phi_{tk,ri}$  between the  $i$ th task reference SSP and the inversion task (with coded location as  $\left( \beta_{tk}^x, \beta_{tk}^y \right)$  and time information as  $\left( \alpha_{tk} \right)$  can be calculated according to equation (1), (2) and (3).

To reduce the negative transfer effect of MTL, we propose a dynamic learning rate adjustment strategy based on the inverse spatio-temporal distance weighted coefficient for task learner training. For the  $i$ th training SSP, the learning rate of task learner  $\eta_{tk,ri}$  will be:

$$\eta_{tk,ri} = \xi \frac{1}{\phi_{tk,ri}} \cdot \frac{1}{\sum_{i=1}^I \frac{1}{\phi_{tk,ri}}} \quad (9)$$

where  $\phi_{tk,ri}$  is calculated by (3) with  $\lambda_{tk,ri} = 0.9$ .

If there are total  $J$  epochs for task learner training, the cost function  $l_{tk} \left( W_{tk}^j \right)$  of the  $j$ th ( $j = 1, 2, \dots, J$ ) batch will be:

$$l_{tk} \left( W_{tk}^j \right) = \frac{1}{2} \sum_{d=1}^D \left( s_{tk,ri}^d - \tilde{s}_{tk,ri}^d \right)^2, \quad (10)$$

where  $\tilde{s}_{tk,ri}^d$  is the inverted SSP related to reference SSP  $S_{tk,ri}$ . Then, the parameter updating of task learner is conducted according to:

$$\dot{W}_{tk}^j = W_{tk}^j - \eta_{tk,ri} \nabla_{W_{tk}^j} l_{tk} \left( W_{tk}^j \right). \quad (11)$$

At last, the converged model will be  $\dot{W}_{tk} = \dot{W}_{tk}^J$ .

When feeding measured sound field information into model  $\dot{W}_{tk}$ , the inverted SSP  $\tilde{S}_{tk}$  can be estimated via once forward propagation.

### 3. Deep-ocean Experiments

#### 3.1. Experimental Settings

To evaluate the feasibility and effectiveness of proposed MTL method for SSP inversion under few-shot learning situation. We conducted deep-ocean experiments at the South Sea of China with areas of  $10km \times 10km$  in middle April 2023, where the depth is about 3500 meters. The relevant data collection corresponding to SSP inversion lasted for a total of 3 days.

The system composition is shown in Fig.3, including 4 anchor nodes, a ship unit that containing a CTD, a set of expendable CTD (XCTD), and an ultra short baseline (USBL) system fixed to the right side of our ship. The anchor nodes and USBL system were used for collecting sonar observation data, while SSP samples were collected by CTD and XCTD.

At the beginning, 4 anchor nodes were sunk in turns to the seabed and their positions were calibrated using signal round-trip propagation time measured by USBL in a circular trajectory. These 4 anchor nodes formed a diamond topology. The real-time position of USBL was located through a ship borne GPS, which was installed near the central axis of the ship. In order to improve the position accuracy of anchor nodes, the lever-arm error between USBL and GPS needs to be corrected. The distance measurement of lever-arm in horizontal direction between the GPS and USBL

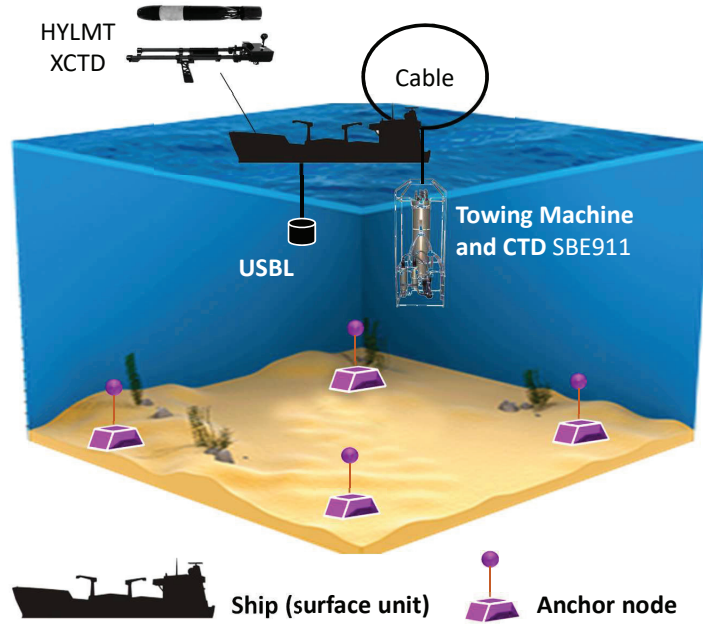


Figure 3: System composition of ocean experiments.

is shown in Fig.4. The horizontal distance was measured in three sections, and the vertical distance was about 18.86 meters (7.5 meters under the water surface) measured under a basically wave free environment in a harbor. Let GPS be the coordinate origin, then the relative coordinates of USBL would be (6.774, 8.392, -18.8603) in meters.

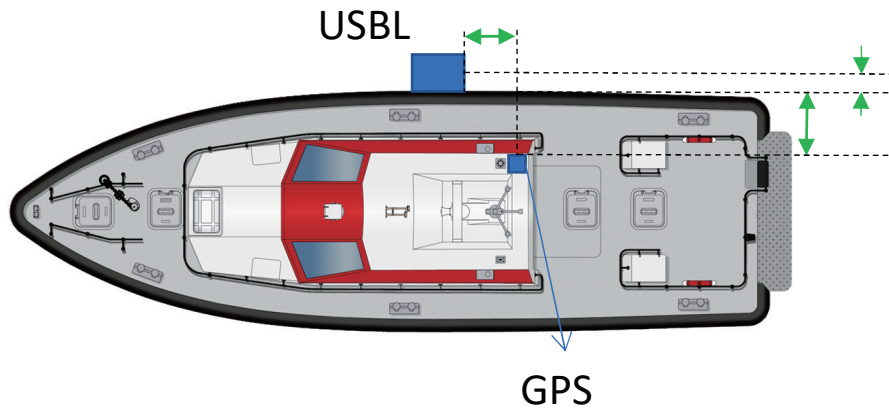


Figure 4: Relative azimuth of GPS and USBL in horizontal direction.

For deploying each anchor node, a full depth of SSP was measured through ship borne CTD, the product model of which is SBE911 produced by Sea-bird Scientific [33]. Considering the high time costs of SSP measurement by CTD (almost 3 hours for once measurement with no ship movement), the XCTDs were adopted to collect the other 9 SSPs, the model of which is HYLMT-2000 produced by [8]. XCTD provides a fast way for SSP measurement that can be performed during ship navigation, and the time cost is related to the measurement depth. For HYLMT-2000 used in this experiment, it takes only about 20 minutes to measure an SSP with maximum depth of 2000 meters. The CTD and XCTD were arranged at the stern of the ship, and the water entry coordinates of CTD and XCTD were measured by the real-time ship borne GPS. These 13 SSPs were collected as reference SSPs. For testing, the last full depth of SSP was measured as an SSP inversion task at the topology center among the 4 anchor nodes. At the same time, the USBL



interacted with four anchor nodes to collect sonar observation data at a period of 8 seconds. The location of anchor nodes and sampled SSPs are shown in Fig.5.

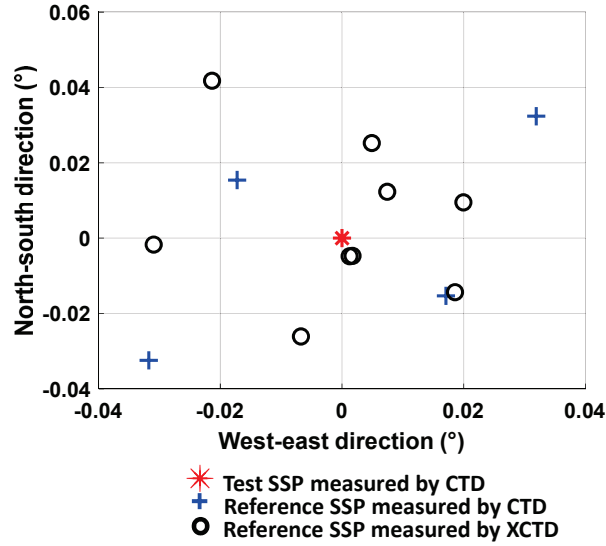


Figure 5: Space distribution of sampled SSPs.

### 3.2. MFP-based SSP Extending

Although XCTD has obvious advantages of time efficiency compared with the SBE911 CTD, the depth coverage of XCTD is limited due to the pressure resistance characteristics of sensors. To tackle this issue, we propose a fast sound speed distribution estimation method based on MFP with EOF decomposition, which is briefly called EOF-PSSP-ME.

The workflow is shown in Fig. 6. There are four steps in EOF-PSSP-ME. Firstly, the original empirical SSPs with full ocean depth are intercepted, forming SSP data with partial depth that is the same as target SSP (to be extended). Secondly, the empirical SSPs with partial and full ocean depth are both decomposed by EOF. Then, the eigenvector coefficients of the target SSP on eigenvectors of empirical SSPs with partial ocean depth are calculated through matching process. Finally, the target SSP with full ocean depth could be constructed by combining the eigenvector coefficients with the eigenvectors of original empirical SSPs. To simplify the model introduction without lose of generality, the SSPs are assumed to have been interpolated at intervals of 1 meter depth.

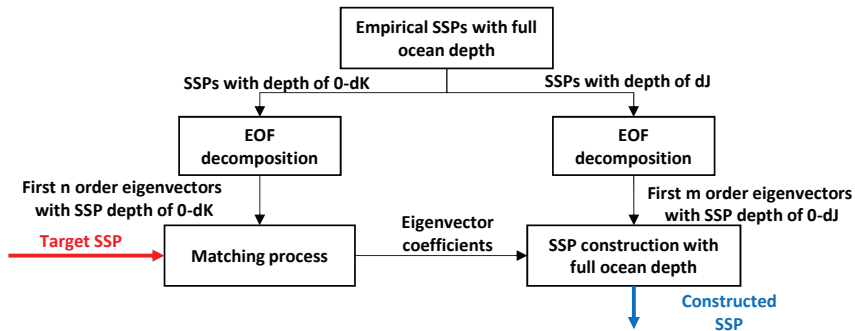


Figure 6: The workflow of EOF-PSSP-ME.

*Empirical SSPs Interception* Let empirical SSPs with full ocean depth form SSP data set  $\mathcal{S} = \{\mathcal{S}_1, \dots, \mathcal{S}_I\}$ , each SSP sample could be expressed as:

$$\mathcal{S}_i = \{(s_{i,0}, d_0), (s_{i,1}, d_1), \dots, (s_{i,j}, d_j)\}, \quad (12)$$

where  $s_{i,j}$  is sound speed,  $d_j$  is depth,  $i = 1, 2, \dots, I$ , means the  $i$ th SSP sample,  $j = 0, 1, \dots, J$  is the index label of depth, and the maximum common depth of SSPs with full ocean depth is  $d_J$ .

If the maximum depth of target SSP to be extended is  $d_K$ , all SSPs in  $\mathcal{S}$  will be partially intercepted by depth and form a data set of reference SSPs  $\bar{\mathcal{S}} = \{\bar{\mathcal{S}}_1, \dots, \bar{\mathcal{S}}_I\}$ ,  $i = 1, 2, \dots, I$  with maximum depth that equals to  $d_K$ .  $\bar{\mathcal{S}}_i$  can be expressed as:

$$\bar{\mathcal{S}}_i = \{(\bar{s}_{i,0}, d_0), (\bar{s}_{i,1}, d_1), \dots, (\bar{s}_{i,k}, d_k)\}, \quad (13)$$

where  $k = 0, 1, \dots, K$ .

*EOF Decomposition* To maintain the original principal component features of any target SSP to be extended, it is necessary to first extract the distribution features of reference SSPs  $\bar{\mathcal{S}}$ , and obtain the components of the target SSP on these distribution features.

The average SSP distribution of  $\bar{\mathcal{S}}$  is:

$$\bar{\mathcal{S}}_{ar,d_K} = \{(\bar{s}_{ar,0}, d_0), (\bar{s}_{ar,1}, d_1), \dots, (\bar{s}_{ar,k}, d_k)\}, \quad (14)$$

where  $\bar{s}_{ar,k}$ ,  $k = 0, 1, \dots, K$  is the average sound speed at depth  $d_k$  that calculated by:

$$\bar{s}_{ar,k} = \frac{1}{I} (\bar{s}_{1,k} + \bar{s}_{2,k} + \dots + \bar{s}_{I,k}). \quad (15)$$

Let  $\mathcal{S}_i^s$  represents the sound speed vector of  $\mathcal{S}_i$  that  $\mathcal{S}_i^s = [s_{i,0}, s_{i,1}, \dots, s_{i,J}]$ . Similarly,  $\bar{\mathcal{S}}_i^s = [\bar{s}_{i,0}, \bar{s}_{i,1}, \dots, \bar{s}_{i,K}]$  and  $\bar{\mathcal{S}}_{ar,d_K}^s = [\bar{s}_{ar,0}, \bar{s}_{ar,1}, \dots, \bar{s}_{ar,K}]$ , where  $K \leq J$ . Then a residual matrix  $\mathcal{S}_{X,d_K}$  of sound speed less than depth  $d_K$  could be constructed as:

$$\mathcal{S}_{X,d_K} = [\bar{\mathcal{S}}_1^s - \bar{\mathcal{S}}_{ar,d_K}^s, \bar{\mathcal{S}}_2^s - \bar{\mathcal{S}}_{ar,d_K}^s, \dots, \bar{\mathcal{S}}_I^s - \bar{\mathcal{S}}_{ar,d_K}^s]. \quad (16)$$

Based on  $\mathcal{S}_{X,d_K}$ , the covariance matrix  $\mathbf{C}_{S,d_K}$  could be derived as:

$$\mathbf{C}_{S,d_K} = \frac{1}{I} \mathcal{S}_{X,d_K} \times \mathcal{S}_{X,d_K}^T, \quad (17)$$

where  $\mathbf{C}_{S,d_K}$  is a matrix with orders of  $(K+1) \times (K+1)$ .

Through EOF decomposition, the matrix of feature values  $\Lambda_{d_K}$  and matrix of feature vectors  $\mathbf{V}_{d_K}$  could be obtained, which satisfies:

$$\mathbf{C}_{S,d_K} \times \mathbf{V}_{d_K} = \mathbf{V}_{d_K} \times \Lambda_{d_K}, \quad (18)$$

In (18),  $\mathbf{V}_{d_K} = [\mathbf{v}_{1,d_K}, \mathbf{v}_{2,d_K}, \dots, \mathbf{v}_{n,d_K}]$ ,  $n = 1, 2, \dots, N$  is a matrix with orders of  $(K+1) \times N$ , and each column represents a feature vector.  $\Lambda_{d_K}$  is an  $N$ -order diagonal matrix that can be expressed as:

$$\Lambda_{d_K} = \begin{bmatrix} \lambda_{1,d_K} & \cdots & 0 \\ \vdots & \ddots & \vdots \\ 0 & \cdots & \lambda_{N,d_K} \end{bmatrix}, \quad (19)$$

where each feature value  $\lambda_{n,d_K}$ ,  $n = 1, 2, \dots, N$  maps to one feature vector  $\mathbf{v}_{N,d_K}$ .

To estimate the full-depth distribution of the target SSP, the feature vectors and values of empirical SSPs with full ocean depth need to be extracted. The average SSP distribution of  $\mathcal{S}$  is:

$$\mathcal{S}_{ar,d_J} = \{(s_{ar,0}, d_0), (s_{ar,1}, d_1), \dots, (s_{ar,j}, d_j)\}, \quad (20)$$

where  $s_{ar,j}, j = 0, 1, \dots, J$  is the average sound speed at depth  $d_j$  that calculated by:

$$s_{ar,j} = \frac{1}{I} (s_{1,j} + s_{2,j} + \dots + s_{I,j}). \quad (21)$$

Similarly to  $\mathbf{S}_{X,d_K}$ , a residual matrix  $\mathbf{S}_{X,d_J}$  of sound speed up to depth  $d_J$  could be constructed as:

$$\mathbf{S}_{X,d_J} = \left[ \mathbf{S}_1^s - \mathbf{S}_{ar,d_J}^s, \mathbf{S}_2^s - \mathbf{S}_{ar,d_J}^s, \dots, \mathbf{S}_I^s - \mathbf{S}_{ar,d_J}^s \right], \quad (22)$$

where  $\mathbf{S}_{ar,d_J}^s = [s_{ar,0}, s_{ar,1}, \dots, s_{ar,J}]$ . The covariance matrix  $\mathbf{C}_{S,d_J}$  could be derived as:

$$\mathbf{C}_{S,d_J} = \frac{1}{I} \mathbf{S}_{X,d_J} \times \mathbf{S}_{X,d_J}^T, \quad (23)$$

where  $\mathbf{C}_{S,d_J}$  is a matrix with orders of  $(J+1) \times (J+1)$ .

Refer to (18), the matrix of feature values  $\Lambda_{d_J}$  and vectors  $\mathbf{V}_{d_J}$  according to empirical SSPs with full ocean depth satisfy:

$$\mathbf{C}_{S,d_J} \times \mathbf{V}_{d_J} = \mathbf{V}_{d_J} \times \Lambda_{d_J}, \quad (24)$$

$\mathbf{V}_{d_J} = [\mathbf{v}_{1,d_J}, \mathbf{v}_{2,d_J}, \dots, \mathbf{v}_{m,d_J}]$ ,  $m = 1, 2, \dots, M$  is a matrix with orders of  $(J+1) \times M$ .  $\Lambda_{d_J}$  is an M-order diagonal matrix that can be expressed as:

$$\Lambda_{d_J} = \begin{bmatrix} \lambda_{1,d_J} & \dots & 0 \\ \vdots & \ddots & \vdots \\ 0 & \dots & \lambda_{M,d_J} \end{bmatrix}. \quad (25)$$

It has been summarized that the difference in SSPs could be represented by combining feature vectors of 3–6 orders. Therefore,  $\mathbf{V}_{d_J}$  and  $\mathbf{V}_{d_K}$  are sorted based on the corresponding feature values in descending order, and the first  $\bar{M}$  or  $\bar{N}$  order's feature vectors are remained, which are denoted as  $\tilde{\mathbf{V}}_{d_J} = [\tilde{\mathbf{v}}_{1,d_J}, \tilde{\mathbf{v}}_{2,d_J}, \dots, \tilde{\mathbf{v}}_{m,d_J}]$ ,  $m = 1, 2, \dots, \bar{M}$  and  $\tilde{\mathbf{V}}_{d_K} = [\tilde{\mathbf{v}}_{1,d_K}, \tilde{\mathbf{v}}_{2,d_K}, \dots, \tilde{\mathbf{v}}_{n,d_K}]$ ,  $n = 1, 2, \dots, \bar{N}$ , where  $3 \leq \bar{M}, \bar{N} \leq 6$ .

**Matching Process** To ensure that the shallow part of reconstructed SSP is consistent with the target SSP, a matching process needs to be performed. Specifically, it is a matching of the target SSP and the combination of feature vectors  $\tilde{\mathbf{V}}_{d_K}$ . By projecting the target SSP onto  $\tilde{\mathbf{V}}_{d_K}$ , the projection coefficient  $\mathbf{c}f_{d_K}$ , which is the combination coefficient of feature vectors, could be obtained. Conversely, the target sample can be restored by combining the coefficient  $\mathbf{c}f_{d_K}$  with  $\tilde{\mathbf{V}}_{d_K}$ .

Let the target SSP be:

$$\mathbf{S}_t = \{(s_{t,0}, d_0), (s_{t,1}, d_1), \dots, (s_{t,k}, d_k)\}, \quad (26)$$

where  $k = 0, 1, \dots, K$ . Then the sound speed vector can be briefly expressed as  $\mathbf{S}_t^s = [s_{t,0}, s_{t,1}, \dots, s_{t,K}]$ , and the residual vector will be  $\mathbf{S}_{X,t} = [\mathbf{S}_t^s - \bar{\mathbf{S}}_{ar,d_K}^s]$ .

Through matching process, the coefficient  $\mathbf{c}f_{d_K}$  could be solved by:

$$\mathbf{c}f_{d_K} = \tilde{\mathbf{V}}_{d_K}^T \cdot \mathbf{S}_{X,t}. \quad (27)$$

**SSP Construction** When combining  $\mathbf{c}f_{d_K}$  and  $\tilde{\mathbf{V}}_{d_J}$ , the target SSP with full ocean depth will be constructed:

$$\hat{\mathbf{S}}_t^s = \mathbf{S}_{ar,d_J}^s + \tilde{\mathbf{V}}_{d_J} \cdot \mathbf{c}f_{d_K}, \quad (28)$$

where  $\hat{\mathbf{S}}_t^s$  will be  $\hat{\mathbf{S}}_t^s = [\hat{s}_{t,0}, \hat{s}_{t,1}, \dots, \hat{s}_{t,J}]$ . Considering depth information, the estimated target SSP can also be expressed as:

$$\hat{\mathbf{S}}_t = \{(\hat{s}_{t,0}, d_0), (\hat{s}_{t,1}, d_1), \dots, (\hat{s}_{t,j}, d_j)\}, \quad (29)$$

where  $j = 0, 1, \dots, J$ .

## 4. Results and Discussions

### 4.1. Preprocessing of SSP Data

For data-driven SSP inversion methods such as EOF-MFP and deep learning, the amount of experimental data collected is relatively small, so the model is prone to be over-fitting. To improve the accuracy of SSP estimation in few-shot learning situations, we propose the MTL model and dynamically adjusting the learning rate during task learner training stage.

As mentioned above, the SSP measured at the center of 4 anchor nodes is used for testing, while the other 13 SSPs are used for task learner training. However, there is still a lack of reference data for multi-task learners to extract common features of sound speed distribution. To solve this problem, 300 historical SSPs (covering at least 3500 meters depth) sampled from the Pacific, Atlantic, and Indian Oceans of the last 10 years are adopted, which are clustered into 10 groups. These SSP data come from the world ocean database 2018 (WOD'18) [3].

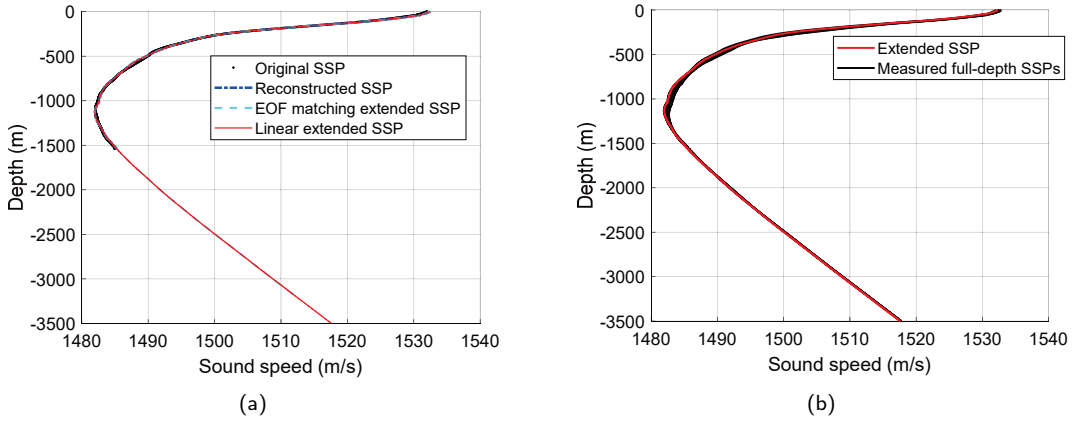


**Figure 7:** SSP extending. (a) An example of SSP extending. (b) An extended SSP and measured full-depth SSPs.

For most SSPs especially those sampled by XCTD, the depth scale can not cover the propagation depth of sonar signal, so the SSPs need to be extended. In this paper, SSP samples are extended through two steps, namely EOF matching extension for SSPs less than 3200 meters depth and linear extension for SSPs more than 3200 meters depth but less than 3500 meters depth. The core idea of EOF matching extension is to maintain the measured results and extend the unmeasured depth portion according to the regional empirical SSP distribution. In EOF matching extension, the full-depth and partial-depth principal components of the empirical SSPs are first extracted separately, and then the projection coefficients are obtained by projecting the measured partial-depth SSP onto the partial-depth principal components, and finally the full-depth SSP is composed of the projection coefficients and the full-depth principal components. Detailed algorithm of EOF matching extension can be referred to our work in [18]. For linear extension, we set the gradient computation window to be 50 meters, and the SSP is linearly extended based on the gradient of the last 50 meters of the measured SSP up to the specified depth. An example of EOF matching extending and linear extending is given in Fig.7.

During the preprocessing of SSPs, SSPs are all standardized and interpolated with a depth spacing of 1 meter, and are finally evenly divided into 50 depth layers to form down-sampled data for being reference data of neural networks.

### 4.2. Performance of MTL

To evaluate the accuracy performance of MTL, the root mean squared error (RMSE) of inverted SSP at the center location of 4 anchors is compared with the real measured SSP. The parameter settings of SL-ML is given in Table 1, and data are processed by 'Matlab 2023a'.

For further comparison of accuracy performance, three state-of-the-art baseline methods are also adopted: spatial interpolation (SIP), EOF-MFP and FNN. For SIP, the proportional weight follows the principle of inverse proportion of spatial distance. For EOF-MFP, the PSO is utilized for searching matching coefficients with 20 particles and 30 iterations, and the order of the principal component is 3. While for FNN, the network structure is the same as the task learner (or any base learner) of MTL, and the learning rate is 0.01, which is equal to that of task learner in MTL.

**Table 1**  
Parameter Settings of SL-ML

Training SSP clusters	10
SSP Clusters per epoch $K$	3
SSPs for multi-task learner training (per cluster) $S_v$	10
Multi-task learner training epochs *	20
Task learner training epochs	20
Task training SSPs per epoch	5
Maximum SSP depth	3500 m
Points of simplified SSPs	50
Learning rate $\alpha$	0.000002
Task learning rate	0.01
Input layer neurons	120
Hidden layer neurons	300
Output layer neurons	50
Factor for task classification $\lambda_{tk}$	0.02
Factor for learning rate adjustment $\lambda_{tk,ri}$	0.9

\* One epoch corresponds to a round of parameter updating, using 3 SSP clusters.

**Table 2**  
RMSE of Inverted SSP by Different Methods

Methods	SIP (m/s)	EOF-MFP (m/s)	FNN (m/s)	MTL (m/s)
Average RMSE	0.3895	0.3341	0.2653	<b>0.2113</b>
0-200 (m)	0.6875	0.5578	0.3366	<b>0.1560</b>
200-800 (m)	0.7529	0.6675	0.2086	<b>0.1930</b>
800-1300 (m)	0.4144	0.3743	0.3232	<b>0.1291</b>
1300-3500 (m)	0.0694	0.0617	0.2567	<b>0.1998</b>

Table 2 gives the average accuracy performance of inverted SSPs with 100 repeated results. It shows that the accuracy of MTL outperforms other state-of-the-art methods under few-shot learning situation, implying that the mapping relationship from sound field data to SSP distribution can be better and faster captured through MTL. An example of inverted SSP is shown in Fig.7.

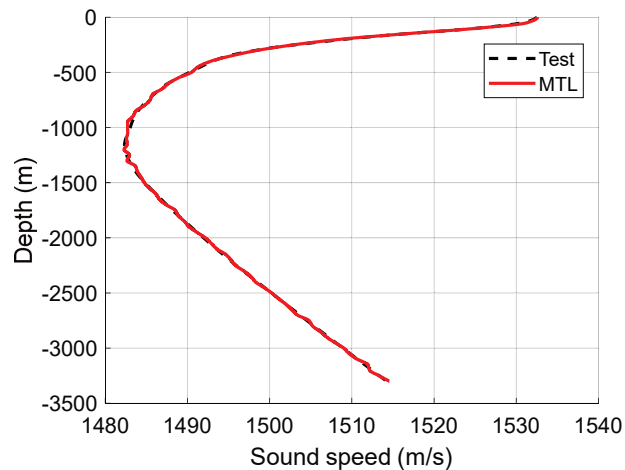


**Figure 8:** An example of inverted SSP.

**Table 3**  
Time Efficiency of Inverted SSP by Different Methods

Methods	SIP	EOF-MFP	FNN	MTL
Inversion stage (s)	0.0033	38.1980	0.0005	0.0008

To illustrate the reason for the fast convergence of MTL, the convergence performance of MTL is compared with that of FNN in Fig.8. After learning different types of SSPs during meta learning stage, the initialization parameters of the task learner in the MTL are closer to the converged parameters, which is beneficial for faster convergence. Moreover, due to prior knowledge of sound speed distribution, the model learning process has less fluctuations, which is conducive to reaching the convergence state faster.

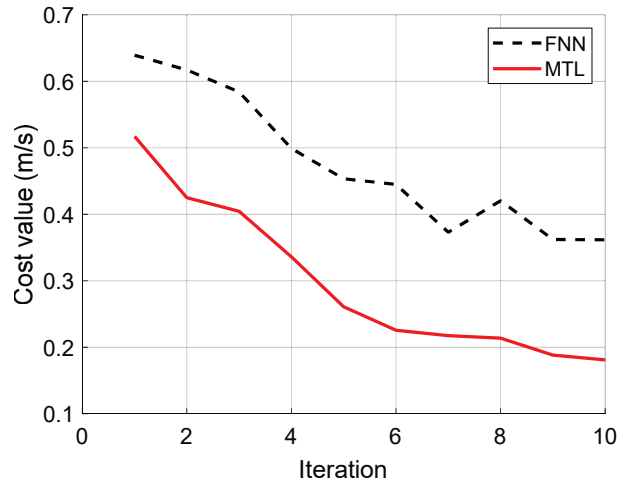


**Figure 9:** Convergence performance of MTL and FNN.

Since the training of neural networks for SSP inversion can be done offline, the time consumption during SSP inversion stage are more noteworthy. The average time consumption of different methods are given in Table 3. MTL inherits the time efficiency advantages of FNN during the inversion stage because it only needs once forward propagation when feeding signal propagation time into the model, and this process can be done by matrix operation.

## 5. Conclusion

In this paper, we propose an MTL method for SSP inversion to improve the accuracy under few-shot learning situations. For verifying the feasibility and effectiveness of the proposed model, a deep-ocean experiment at the South China Sea was conducted in April 2023. Through verification on real sampled SSP data and sonar observation data, it is shown that the proposed MTL has better accuracy performance in few-shot learning SSP construction issues, and inherits the high time efficiency of neural networks during the inversion stage.

## Conflict of Interest Statement

The authors declare that the research was conducted in the absence of any commercial or financial relationships that could be construed as a potential conflict of interest.

## References

- [1] Alet, F., Schneider, M.F., Lozano-Perez, T., Kaelbling, L.P., 2020. Meta-learning curiosity algorithms, in: Eighth International Conference on Learning Representations (ICLR), OpenReview.net, USA. pp. 1–22. doi:10.48550/arXiv.2003.05325.

- [2] Bianco, M.J., Gerstoft, P., Traer, J., Ozanich, E., Roch, M.A., Gannot, S., Deledalle, C.A., 2019. Machine learning in acoustics: theory and applications. *Journal of the Acoustical Society of America* 146, 3590–3628.
- [3] Boyer, T., Baranova, O., Coleman, C., Garcia, H., Grodsky, A., Locarnini, R.A. and Mishonov, A., Paver, C., Reagan, J., Seidov, D., Smolyar, I., Weathers, K., Zweng, M., 2021. World ocean database 2018. <https://www.ncei.noaa.gov/access/world-ocean-database/datawodgeo.html>.
- [4] Carroll, P., Mahmood, K., Zhou, S., Zhou, H., Xu, X., Cui, J.H., 2014. On-demand asynchronous localization for underwater sensor networks. *IEEE transactions on signal processing* 62, 3337–3348. doi:10.1109/TSP.2014.2326996.
- [5] Chang, H., Han, J., Zhong, C., Snijders, A.M., Mao, J., 2018. Unsupervised transfer learning via multi-scale convolutional sparse coding for biomedical applications. *IEEE Transactions on Pattern Analysis and Machine Intelligence* 40, 1182–1194.
- [6] Choo, Y., Seong, W., 2018. Compressive sound speed profile inversion using beamforming results. *Remote Sensing* 10, 1–18. doi:10.3390/rs10050704.
- [7] Cobbe, K., Klimov, O., Hesse, C., Kim, T., Schulman, J., 2019. Quantifying generalization in reinforcement learning, in: Chaudhuri, K., Salakhutdinov, R. (Eds.), *Proceedings of the 36th International Conference on Machine Learning*, PMLR, New York, USA. pp. 1282–1289. doi:10.48550/arXiv.1812.02341.
- [8] Electronics, H., 2023. Hylmt-xctd. <http://www.haiyanec.com/hlgcsb/358>.
- [9] Elsken, T., Metzen, J.H., Hutter, F., 2019. Neural architecture search: A survey. *J. Mach. Learn. Res.* 20, 1997–2017. doi:10.5555/3322706.3361996.
- [10] Erol-Kantarci, M., Mouftah, H.T., Oktug, S., 2011. A survey of architectures and localization techniques for underwater acoustic sensor networks. *IEEE Communications Surveys & Tutorials* 13, 487–502. doi:10.1109/SURV.2011.020211.00035.
- [11] Fengzhong, Q., Shiyuan, W., Zhihui, W., Zubin, L., 2016. A survey of ranging algorithms and localization schemes in underwater acoustic sensor network. *China Communications* 13, 66–81. doi:10.1109/CC.2016.7445503.
- [12] Finn, C., Abbeel, P., Levine, S., 2017. Model-agnostic meta-learning for fast adaptation of deep networks, in: *Proceedings of the 34th International Conference on Machine Learning (ICML'17) - Volume 70*, JMLR.org, Cambridge, MA, USA. p. 1126–1135.
- [13] Goodfellow, I., Bengio, Y., Courville, A., 2016. *Deep Learning*. MIT Press, Cambridge, Massachusetts, USA.
- [14] Hospedales, T., Antoniou, A., Micaelli, P., Storkey, A., 2022. Meta-learning in neural networks: A survey. *IEEE Transactions on Pattern Analysis and Machine Intelligence* 44, 5149–5169. doi:10.1109/TPAMI.2021.3079209.
- [15] Huang, W., Li, D., Jiang, P., 2018. Underwater sound speed inversion by joint artificial neural network and ray theory, in: *Proceedings of the Thirteenth ACM International Conference on Underwater Networks & Systems (WUWNet'18)*, ACM, ACM, New York, NY, USA. pp. 1–8. doi:10.1145/3291940.3291972.
- [16] Huang, W., Li, D., Xu, T., Gao, F., 2023a. A fast estimation method for sound velocity distribution based on cross spatiotemporal sound velocity profile clustering. Patent No. 202211243606.9 (CN), Filed October 12th., 2022, Issued February. 3rd., 2023.
- [17] Huang, W., Liu, M., Li, D., Yin, F., Chen, H., Zhou, J., Xu, H., 2021. Collaborating ray tracing and ai model for auv-assisted 3-d underwater sound-speed inversion. *IEEE Journal of Oceanic Engineering* 46, 1372–1390.
- [18] Huang, W., Lu, J., Li, S., Xu, T., Wang, J., Zhang, H., 2023b. Fast estimation of full depth sound speed profile based on partial prior information, in: *IEEE International Conference on Electronic Information and Communication Technology (in press)*, IEEE, New York, USA. pp. 1–6.
- [19] Jensen, F.B., Kuperman, W.A., Porter, M.B., Schmidt, H., 2011. *Computational ocean acoustics: Chapter 1*. Springer Science & Business Media, New York, NY, USA. doi:10.1008/978-1-4419-8678-8.
- [20] Jin, G., Liu, F., Wu, K., Chen, C., 2020. Deep learning-based framework for expansion, recognition and classification of underwater acoustic signal. *Journal of Experimental and Theoretical Artificial Intelligence* 32, 205–218.
- [21] Komen, D.F.V., Neilsen, T.B., Howarth, K., Knobles, D.P., Dahl, P.H., 2020. Seabed and range estimation of impulsive time series using a convolutional neural network. *The Journal of the Acoustical Society of America* 147, 403–408.
- [22] Li, Q., Shi, J., Zhenglin, L., Yu, L., Zhang, K., 2019. Acoustic sound speed profile inversion based on orthogonal matching pursuit. *Acta Oceanologica Sinica* 38, 149–157.
- [23] Liu, J., Wang, Z., Cui, J.H., Zhou, S., Yang, B., 2015. A joint time synchronization and localization design for mobile underwater sensor networks. *IEEE Transactions on Mobile Computing* 15, 530–543. doi:10.1109/TMC.2015.2410777.
- [24] Luo, J., Yang, Y., Wang, Z., Chen, Y., 2021. Localization algorithm for underwater sensor network: A review. *IEEE Internet of Things Journal* 8, 13126–13144. doi:10.1109/JIOT.2021.3081918.
- [25] Michalopoulou, Z.H., Alexandrou, D., De Moustier, C., 1993. Application of neural and statistical classifiers to the problem of seafloor characterization. *IEEE Journal of Oceanic Engineering* 20, 190–197.
- [26] Munk, W., Wunsch, C., 1979. Ocean acoustic tomography: A scheme for large scale monitoring. *Deep Sea Research Part A. Oceanographic Research Papers* 26, 123–161. doi:10.1016/0198-0149(79)90073-6.
- [27] Munk, W., Wunsch, C., 1983. Ocean acoustic tomography: Rays and modes. *Reviews of Geophysics* 21, 777–793. doi:10.1029/RG021i004p00777.
- [28] Pan, S.J., Yang, Q., 2010. A survey on transfer learning. *IEEE Transactions on Knowledge and Data Engineering* 22, 1345–1359.
- [29] Piccolo, J., Haramuniz, G., Michalopoulou, Z.H., 2019. Geoacoustic inversion with generalized additive models. *The Journal of the Acoustical Society of America* 145, 463–468.
- [30] Pérez-Rúa, J.M., Zhu, X., Hospedales, T., Xiang, T., 2020. Incremental few-shot object detection, in: *2020 IEEE/CVF Conference on Computer Vision and Pattern Recognition (CVPR)*, IEEE, USA. pp. 13843–13852. doi:10.1109/CVPR42600.2020.01386.
- [31] Rich, C., 1997. Multitask learning. *Machine Learning* 28, 41–75. doi:10.1023/A:1007379606734.
- [32] Rumelhart, D.E., Hinton, G.E., Williams, R.J., 1986. Learning representations by back propagating errors. *Nature* 5, 533–536. doi:10.1038/323533a0.
- [33] Scientific, S.B., 2023. Sbe 911plus ctd. <https://www.seabird.com/sbe-911plus-ctd/product?id=60761421595>.

- [34] Shang, E., 1989. Ocean acoustic tomography based on adiabatic mode theory. *The Journal of the Acoustical Society of America* 85, 1531–1537. doi:10.1121/1.397355.
- [35] Snell, J., Swersky, K., Zemel, R., 2017. Prototypical networks for few-shot learning, in: *Proceedings of the 31st International Conference on Neural Information Processing Systems*, Curran Associates Inc., Red Hook, NY, USA. p. 4080–4090. doi:10.5555/3294996.3295163.
- [36] Stephan, Y., Thiria, S., Badran, F., 1995. Inverting tomographic data with neural nets, in: *'Challenges of Our Changing Global Environment'. Conference Proceedings. OCEANS'95 MTS/IEEE*, IEEE, New York, USA. pp. 1501–1504. doi:10.1109/OCEANS.1995.528711.
- [37] Sun, W.C., Bao, J.Y., Jin, S.H., Xiao, F.M., Cui, Y., 2016. Inversion of sound velocity profiles by correcting the terrain distortion. *Geomatics and Information Science of Wuhan University* 41, 349–355. doi:10.13203/j.whugis20140142.
- [38] Tang, J.f., Yang, S.e., 2006. Sound speed profile in ocean inverted by using travel time. *Journal of Harbin Engineering University (In Chinese)* 27, 733–737. doi:10.3969/j.issn.1006-7043.2006.05.022.
- [39] Tolstoy, A., Diachok, O., Frazer, L., 1991. Acoustic tomography via matched field processing. *The Journal of the Acoustical Society of America* 89, 1119–1127. doi:10.1121/1.400647.
- [40] Vanschoren, J., 2018. Meta-learning: A survey. arXiv:1810.03548v1, 1–29doi:10.48550/arXiv.1810.03548.
- [41] Weiss, K., Khoshgoftaar, T.M., Wang, D., 2016. A survey of transfer learning. *Journal of Big Data* 3, 1–40.
- [42] Wu, Q., Xu, W., 2017. Matched field source localization as a multiple hypothesis tracking problem, in: *Proceedings of the International Conference on Underwater Networks & Systems (WUWNet'17)*, ACM, New York, NY, USA. pp. 1–2. doi:10.1145/3148675.3148723.
- [43] Yang, Y., Hospedales, T.M., 2017. Deep multi-task representation learning: A tensor factorisation approach, in: *International Conference on Learning Representations (ICLR)*, OpenReview.net, USA. pp. 1–12. URL: <https://openreview.net/forum?id=SkhU2fc11>, doi:10.48550/arXiv.1605.06391.
- [44] Yosinski, J., Clune, J., Bengio, Y., Lipson, H., 2014. How transferable are features in deep neural networks?, in: *Proceedings of the 27th International Conference on Neural Information Processing Systems - Volume 2*, MIT Press, Cambridge, MA, USA. p. 3320–3328. doi:10.48550/arXiv.1411.1792.
- [45] Zhang, M., Xu, W., Xu, Y., 2015. Inversion of the sound speed with radiated noise of an autonomous underwater vehicle in shallow water waveguides. *IEEE Journal of Oceanic Engineering* 41, 204–216. doi:10.1109/OJE.2015.2418172.
- [46] Zhang, W., Yang, S.e., Huang, Y.w., Li, L., 2012. Inversion of sound speed profile in shallow water with irregular seabed, in: *Advances in Ocean Acoustics: Proceedings of the 3rd International Conference on Ocean Acoustics (OA2012)*, AIP, Melville, NY, USA. pp. 392–399. doi:10.1063/1.4765934.
- [47] Zhang, Z.M., 2005. The Study for Sound Speed Inversion in Shallow Water on Application of Genetic and Simulated Annealing Algorithms. Master's thesis, chapter 4. Harbin Engineering University. Harbin, China. doi:10.7666/d.y780567.
- [48] Zheng, G.Y., Huang, Y.W., 2017. Improved perturbation method for sound speed profile inversion. *Journal of Harbin Engineering University (in Chinese)* 38, 371–377. doi:10.11990/jheu.201603075.